

Research Article

Uplink Spectrum Overlay Coverage Enhancement Algorithm in 5G Network

Jian-feng Jiang¹ and Hui-jie Ding² 

¹Suzhou Industrial Park Institute of Services Outsourcing, Suzhou 215123, China

²School of Artificial Intelligence, The Open University of Guangdong, Guangzhou 510091, China

Correspondence should be addressed to Hui-jie Ding; 811054@qq.com

Received 13 September 2021; Accepted 22 October 2021; Published 22 December 2021

Academic Editor: Kim-Hua Tan

Copyright © 2021 Jian-feng Jiang and Hui-jie Ding. This is an open access article distributed under the Creative Commons Attribution License, which permits unrestricted use, distribution, and reproduction in any medium, provided the original work is properly cited.

The imbalance between the uplink and downlink rates and coverage of the 5G network has led to limited vertical industry services. Aiming at breaking the imbalance between the uplink and downlink rates and improving the coverage of 5G network, a uplink coverage enhancement algorithm is designed from the aspects of networking mode, bandwidth, uplink and downlink subframe ratio, etc. It uses high- and low-frequency time-frequency joint scheduling to enable uplink full-time slot scheduling, thereby improving uplink coverage and rate. According to the actual test on the live network, the results show that the super-uplink algorithm can increase the near-point uplink rate by 15% to 30%, increase the uplink rate for indoor midpoint scenarios by 40% to 80%, and increase the uplink rate for outdoor and indoor weak spot scenarios by 100% to 400%.

1. Introduction

When redefining 5G networks guided by industry needs, the 2C market has mainly high speed and the current 5G network speed can easily reach more than 1 Gpbs downstream, which is fast enough to meet the market demand. However, in the 2B market, vertical industries have put forward new requirements for upstream speeds and latency has become the most important requirement. For example, the demand for uplink speed of the smart mining factory has reached more than 100 Mbps, and the end-to-end delay requirement is less than 15 ms. The 5 G uplink rate is limited by multiple factors such as terminals, networks, and frequency spectrum, which make it difficult to meet the uplink rate requirements of vertical industries. The transmitting power of the terminal is much smaller than the transmitting power of the base station, and the difference between the two powers is nearly a thousand times. In the mainstream time slot ratio of 7 : 3, 4 : 1, or 8 : 2, the uplink proportion is very small. At present, the C-band propagation loss in the mainstream 5G frequency band is huge and the penetration loss of 3.5 GHz in a typical wall is as high as 26 dB.

As the 5G network is still mainly for mass services at this stage, the time slot ratio is still dominated by downlink time slots [1, 2]. The difference in uplink and downlink coverage is huge, and the uplink coverage is obviously limited [3–5]. In the deployment of vertical industry applications, its uplink coverage and speed are a major requirement. How to solve the combination of 5G high- and low-frequency spectrum is a hot issue of current research. Commercial use of 5G networks only started at the end of 2019. In the early stage of 5G network operation, the literature [4] proposed using 4G and 5G co-site strategies to increase the uplink rate. However, due to the high frequency band and low time slot of the network, the uplink coverage of the 5G network is not continuous [6]. The study in [7] proposes to use spectrum aggregation technology to solve the uplink and downlink access of 5G heterogeneous networks, but it cannot completely solve the problem of cell handover [8, 9]. The study in [10] uses link adaptation algorithms to control the uplink channel power, which can optimize the uplink to a certain extent, but it cannot solve the essential problem. In view of the above problems, the algorithm in this paper realizes the complementarity of

FDD uplink time slot and TDD uplink time domain and improves uplink coverage and throughput.

In terms of the 3.5 GHz high-frequency site, China Telecom also has 1.8/2.1 GHz low-frequency sites. The number of sites nationwide is about 60,000, and the load is low. Therefore, incorporating the 1.8/2.1 GHz frequency band into 5G network construction can obtain greater uplink and downlink advantages.

2. Analysis of 5G Network Uplink and Downlink Coverage

2.1. 5G Spectrum. Spectrum is the core resource in the field of mobile communications [11, 12]. The 5G NR (new radio) spectrum defined by the 3GPP standard mainly includes sub-6 GHz (410–7 125 MHz) and millimeter wave (24 250–52 600 MHz). It has multiple modes such as frequency division duplex (FDD), time division duplex (TDD), and supplementary uplink (SUL). At present, commercial 5G networks mainly use the TDD mode 3.5 GHz and 2.6 GHz frequency bands. Compared with the 1.8 GHz and 2.1 GHz frequency bands used by 4G FDD networks, they have a large bandwidth advantage. Its single-user peak rate is significantly higher than of 4G under the condition of low path loss, but the penetration loss is higher. The uplink and downlink time slot ratios of commercial 5G networks are 3 : 7, 1 : 4, or 2 : 8, and the available uplink time slots are relatively small. Table 1 is the spectrum information status of today's operators.

2.2. Uplink and Downlink Rate. The application of 5G network's large bandwidth and large-scale array antenna gain has greatly improved the rate of 5G network compared with that of 4G networks. Under ideal conditions, the downlink rate of 5G networks is as high as 1.2 Gbps, which is about 10 times the rate of 4G networks. The uplink rate is as high as 130 Mbps, which is about 4 times the rate of the 4G network. However, in a nonideal state, when the 5G network RSRP is at the coverage edge of -110 dBm to -120 dBm, the downlink rate can be maintained at 100 to 300 Mbps and the minimum uplink rate is only about 2.58 Mbps. The uplink and downlink rates are shown in Figure 1.

3. Uplink Coverage Enhancement Algorithm

3.1. Principles of Coverage Enhancement Algorithm. The uplink coverage enhancement algorithm uses NR FDD to enhance uplink coverage, experience, and capacity. The FDD frequency band is low, the coverage is strong, and the frequency division duplex transmission has no additional waiting delay, but the transmission bandwidth is small. The TDD frequency band has a large bandwidth, and the uplink and the downlink both use mature applications of MIMO technology. Under the premise of the same subcarrier spacing, the coverage and delay are weaker than FDD. Coverage enhancement algorithm technology realizes the uplink transmission of FDD NR and TDD NR, as the principle shown in Figure 2.

Taking the influence of signal coverage in high-frequency band and low-frequency band into account, there are two situations in the time slot scheduling—the mid-near-point area and the far-point area. In the mid-near-point area, the algorithm mainly improves the uplink capacity and user experience. In the far-point area, the algorithm mainly improves the C-band 3.5 GHz coverage. In this way, the Sub-3 GHz spectrum is fully utilized to realize 5G full-time slot scheduling.

3.2. Design of Uplink Coverage Enhancement Algorithm

3.2.1. The First Step: User (UE) Access. The UE is in idle mode when it is powered on and accesses the user equipment in the 3.5 GHz frequency band. Currently, most 5G mobile phone chips support 5G networks, and the UE can dynamically change the configuration. When the UE is at the edge of the 5G network, the network uplink coverage is limited and the 5G network controls the UE to access the PUSCH of the Sub-3G network for data transmission. The basis for judging whether the 5G uplink coverage is limited is the 5G uplink SINR. When the SINR is greater than the threshold, it indicates that the uplink coverage is good and the C-band network is selected. When the SINR is less than the threshold, the Sub-3G network is selected. The process is shown in Figure 3.

3.2.2. The Second Step: Allocation of Uplink Frequency-Domain Resource. The PUSCH is configured with two frequency bands, C-band and Sub-3G, and the PUCCH is configured with only C-band. The process is shown in Figure 4. According to the latest 5G R16 standard, DCI formats indicate whether the DCI information is uplink or downlink scheduling information. It occupies 1 bit, a value of 0 indicates uplink, and a value of 1 indicates downlink. The uplink DCI mainly indicates uplink PUSCH transmission, including two types of field information of DCI format 0_0 and DCI format 0_1.

When the field information is DCI format 0_0, if DCI format 0_0 is scrambled by C-RNTI or CS-RNTI or MCS-C-RNTI, the number of bits occupied by frequency domain resources is calculated by the following formula:

$$\left\lceil \log_2 \left(N_{\text{RB}}^{\text{UL,BWP}} \frac{N_{\text{RB}}^{\text{UL,BWP}} + 1}{2} \right) \right\rceil, \quad (1)$$

$$\left\lceil \log_2 \left(N_{\text{RB}}^{\text{UL,BWP}} \frac{N_{\text{RB}}^{\text{UL,BWP}} + 1}{2} \right) \right\rceil - N_{\text{UL,HOP}}. \quad (2)$$

When PUSCH frequency hopping is used, $N_{\text{RB}}^{\text{UL,BWP}}$ is the size of the activated UL BWP. For the uplink resource allocation type is 1, the PDSCH is used for frequency hopping situation, $N_{\text{UL,HOP}}$ is the number of bits which is used to indicate frequency offset. If the frequency hopping offset list contains 2 offset values, $N_{\text{UL,HOP}}$ is set to 1. If the frequency hopping offset list contains 4 offset values, $N_{\text{UL,HOP}}$ is set to 2. At this time, formula (2) is used to calculate the number of remaining bits to indicate frequency-domain resource

TABLE 1: Comparative analysis of operators' existing spectrum resources.

| | China Mobile (MHz) | China Telecom | China Unicom (MHz) |
|-----------|--------------------|--------------------------|--------------------|
| 4.9 (GHz) | 100 | | |
| 3.5 | | 100 MHz | |
| 2.6 | 160 | | |
| 2.1 | | $2 \times (20 + 10)$ MHz | 100 |

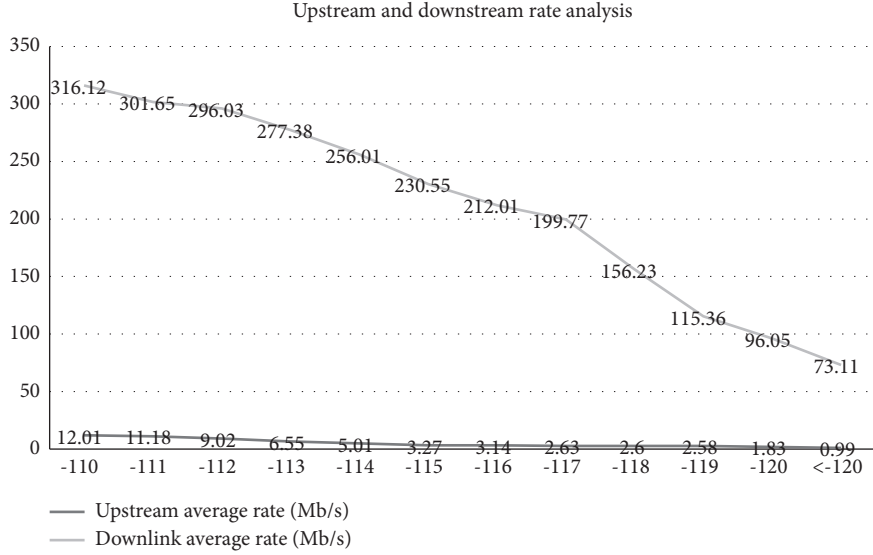


FIGURE 1: Comparison of the average uplink and downlink rate at the edge of network coverage.

allocation. Since the uplink resource allocation type is 1 and the PDSCH frequency hopping is not used, the number of bits calculated by the formula (1) indicates the frequency-domain resource allocation.

When DCI format 0_0 is scrambled by TC-RNTI, $N_{\text{RB}}^{\text{UL,BWP}}$ in formula (1) is the size of the initial UL BWP. If its value is less than 50, then $N_{\text{UL,HOP}}$ is set to 1; otherwise, $N_{\text{UL,HOP}}$ is set to 2.

When the local segment information is DCI format 0_1, the cross-domain carrier scheduling feature is enabled and the carrier indicator field is generated.

When the field information is 0 bits, it indicates the current cell, and when the field information is 3 bits, it indicates the corresponding cell. The frequency-domain

resource allocation field N_{RBG} indicates the total number of UL BWP RBGs, and the calculation formula is shown in

$$N_{\text{RBG}} = \left\lceil \frac{(N_{\text{BWP},i}^{\text{start}} + N_{\text{BWP},i}^{\text{size}}) \bmod P}{P} \right\rceil. \quad (3)$$

In formula (3), P represents all other RBG sizes, and the first RBG size is calculated by the following formula:

$$\text{RBG}_0^{\text{size}} = P - N_{\text{BWP},i}^{\text{start}} \bmod P. \quad (4)$$

If $(N_{\text{BWP},i}^{\text{start}} + N_{\text{BWP},i}^{\text{size}}) \bmod P$ is greater than 0, the last RBG size calculation formula is as follows:

$$\text{RBG}_{\text{last}}^{\text{size}} = \begin{cases} (N_{\text{BWP},i}^{\text{start}} + N_{\text{BWP},i}^{\text{size}}) \bmod P, & (N_{\text{BWP},i}^{\text{start}} + N_{\text{BWP},i}^{\text{size}}) \bmod P > 0, \\ P, & \text{otherwise.} \end{cases} \quad (5)$$

If uplink resource allocation type 1 is configured, the value of this field is calculated by formula (1). The $N_{\text{RB}}^{\text{UL,BWP}}$ is the size of the activated UL BWP. If both of uplink resource allocation type 0 and type 1 are configured, the value of this field is calculated by

$$\max \left(\left\lceil \log_2 \left(\frac{N_{\text{RB}}^{\text{UL,BWP}} (N_{\text{RB}}^{\text{UL,BWP}} + 1)}{2} \right) \right\rceil, N_{\text{RBG}} \right) + 1. \quad (6)$$

The uplink resource allocation type is 0, and the value of N_{RBG} indicates frequency-domain resource allocation. The uplink resource allocation type is 1, and the value calculated by formula (1) indicates frequency-domain resource allocation. When it uses PDSCH for frequency hopping, the frequency hopping offset list contains 2 offset values and $N_{\text{UL,HOP}}$ is set to 1. If the frequency hopping offset list contains 4 offset values, $N_{\text{UL,HOP}}$ is set to 2. At this time, formula (2) is used to calculate the number of remaining bits to indicate

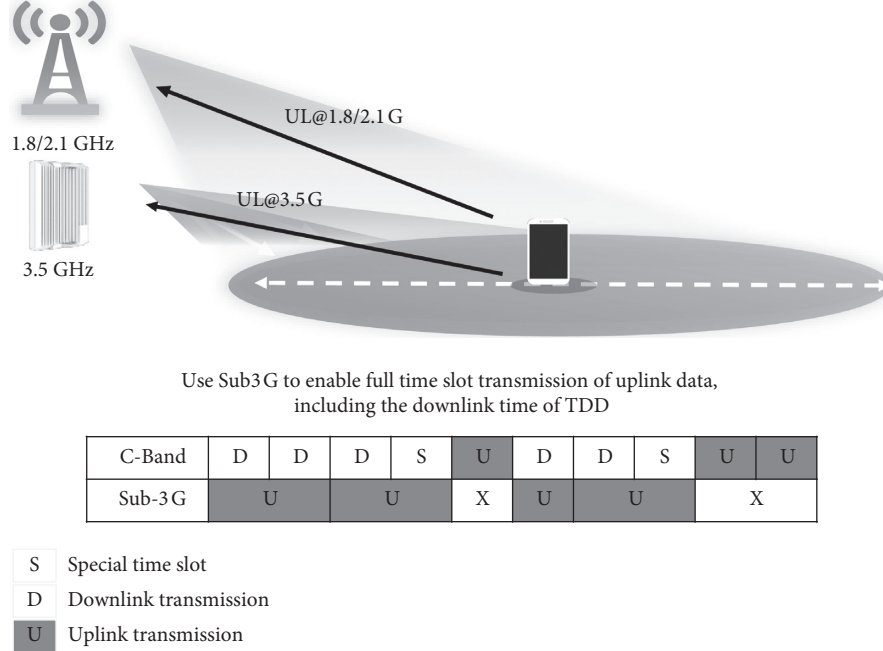


FIGURE 2: Principle of uplink coverage enhancement.

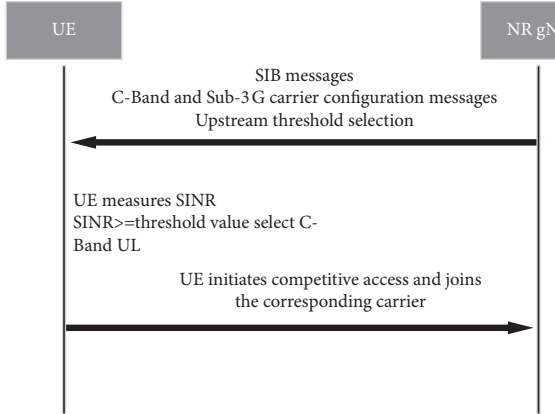


FIGURE 3: User access.

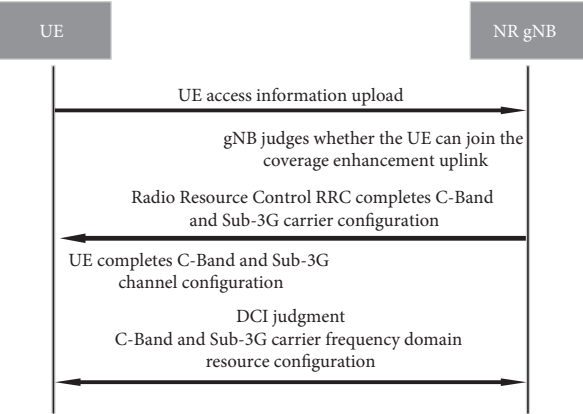


FIGURE 4: Channel configuration.

frequency-domain resource allocation. The uplink resource allocation type is 1, the PDSCH frequency hopping situation is not used, and the value calculated by formula (1) is used to indicate frequency-domain resource allocation.

3.2.3. The Third Step: Cell Handover. When the UE is moving, the coverage enhancement NR spectrum and the cell handover process are as shown in Figure 5.

3.2.4. The Fourth Step: Uplink Time-Domain Resource Scheduling. The base station performs uplink data time slot scheduling, which is determined by the time-domain resource assignment field in DCI format 1_0 and DCI format 1_1. The value m of the field time-domain resource assignment is used to determine the row index $m+1$ in the

time-domain resource assignment table. The allocation position of the PUSCH time slot is calculated by

$$\left\lfloor n * \frac{2^u \text{PUSCH}}{2^u \text{PDCCH}} \right\rfloor + k_0. \quad (7)$$

Here, n is the time slot for scheduling DCI, k_0 is the time slot offset based on PDCCH receiving PUSCH, and 2^uPUSCH and 2^uPDCCH are configured subcarrier intervals. The start and length indicator SLIV determines the number of start symbols S and consecutive symbols L in the PUSCH time domain.

$$\text{SLIV} = \begin{cases} 14 * (L - 1) + S, & L - 1 \leq 7, \\ 14 * (14 - L + 1) + (14 - 1 - S), & \text{otherwise.} \end{cases} \quad (8)$$

Here, $0 < L \leq 14 - S$. The base station performs time-domain scheduling through DCI, and the scheduling algorithm in the mid-near-point area and the far-point area are shown in Figure 6.

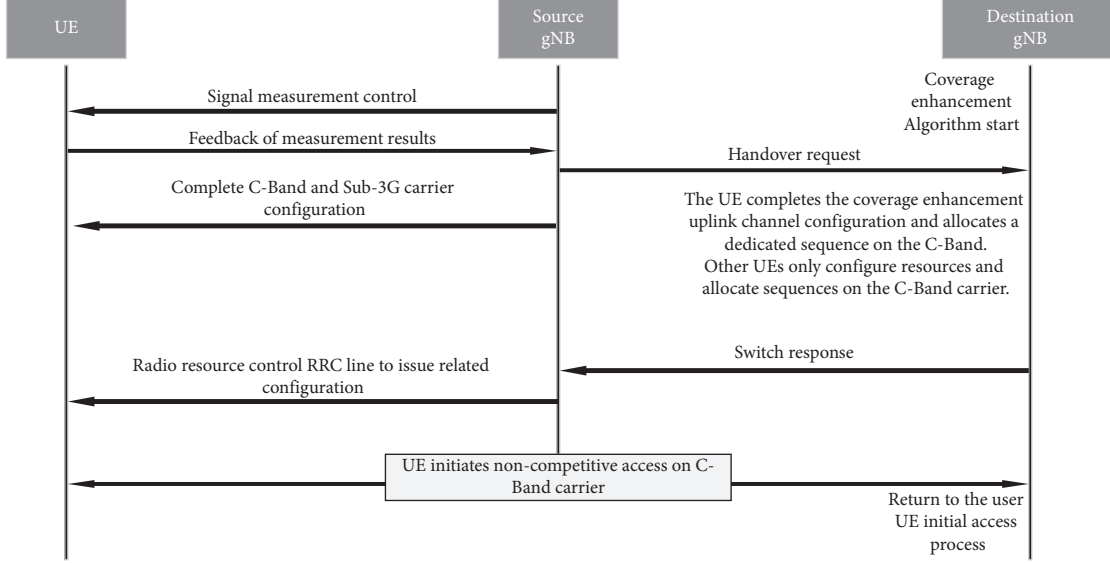


FIGURE 5: Cell handover process.

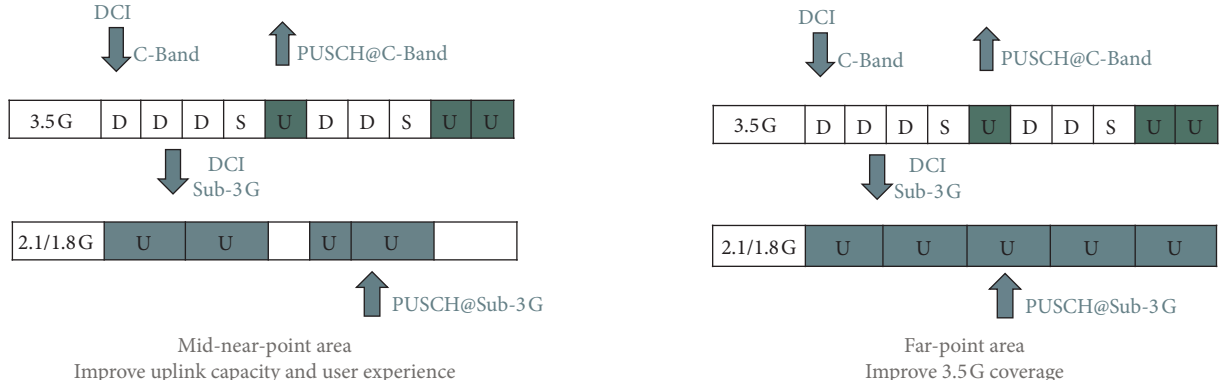


FIGURE 6: Two types of regional time-domain scheduling.

4. Network Emulation

4.1. Uplink Equivalent Bandwidth Comparison. In the actual network environment, the uplink performance comparison of different locations is tested by selecting the network spectrum of different operators and setting the equivalent bandwidth. The test environment is shown in Table 2.

The test result is shown in Figure 7. The uplink coverage enhancement algorithm in the 3.5 G + 2.1 G network has a near-point area uplink resource utilization rate of 100%, which improves the uplink capacity and experience by 30%. In far-point areas, the uplink coverage enhancement algorithm uses 2.1 G uplink resources to increase the 3.5 G coverage rate by 100%.

4.2. Fixed-Point Test. The test scenario is selected as a mining area in the industrial Internet field of the vertical industry. The main coverage direction of the opened sectors is the mining area, which is a basin topography, and the lowest platform is flat. Fixed-point test scenario Area 1 is about 325

meters away from the station horizontally, Area 2 is about 505 meters away from the station horizontally, and Area 3 is about 630 meters away from the station horizontally. The station and terminal configuration parameters are shown in Table 3.

The test data are shown in Table 4.

The test results are shown in Figure 8. The uplink coverage enhancement algorithm uses high- and low-frequency time-frequency joint scheduling and 3.5 G + 2.1 G uplink full-slot scheduling, and the rate is improved. The use of 2.1 G frequency band to spread data in weak coverage areas can reduce loss and enhance TDD uplink coverage.

From the statistics, we can see that in the near-point peak scenario, after the uplink coverage enhancement algorithm is executed, the uplink rate is increased by about 20%. In the outdoor midpoint scenario, after the uplink coverage enhancement algorithm is executed, the uplink rate is increased by 40% to 80%. In outdoor weak coverage scenarios, after the uplink coverage enhancement algorithm is executed, the uplink rate is increased by 100% to 400%.

TABLE 2: Horizontal comparison parameters.

| Uplink algorithm | Spectrum bandwidth |
|---|-----------------------------|
| China Mobile | 2.6 G(20M)@2T |
| China Telecom | 3.5 G(30M)@2T |
| China Telecom uplink coverage enhancement | 3.5 G(30M)@2T&2.1 G(14M)@1T |

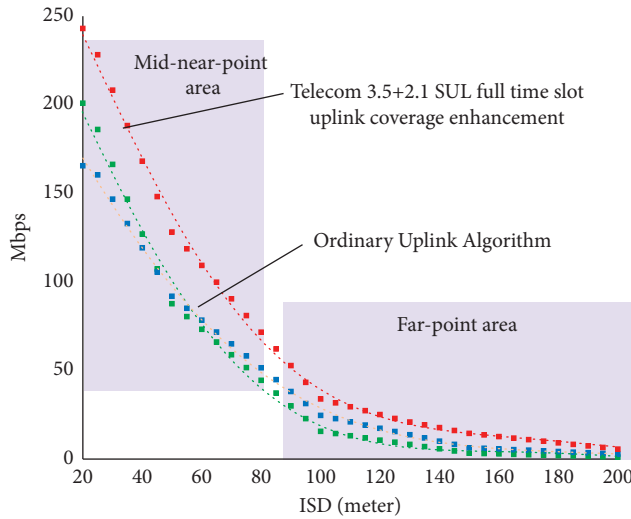


FIGURE 7: Horizontal performance comparison.

TABLE 3: Uplink coverage enhancement algorithm test site and terminal parameter configuration.

| Parameter | NR TDD 3.5 G | Uplink coverage enhancement 3.5 G + 2.1 G |
|-------------------------------------|---------------|---|
| Uplink bandwidth | 100 MHz | 3.5 G 100 MHz + 2.1 G 20 MHz |
| Uplink and downlink time slot ratio | 7:3 | NA |
| Base station antenna | 64R | 4R |
| Base station power | 200 W | 200 W |
| Terminal type | CPE PRO | |
| Terminal antenna | 2T4R | 3.5 G 2T + 2.1 G 1T |
| Frequency range | 3400~3500 MHz | 1920~1940 MHz |

TABLE 4: Test data of the mining area.

| Test area | Test location | SSB-RSRP (dBm) | NR 3.5 G TDD uplink rate (Mbps) | Coverage-enhanced uplink rate (Mbps) | Uplink gain (%) |
|-----------|---------------|----------------|---------------------------------|--------------------------------------|-----------------|
| Area 1 | P1 | -75.77 | 234.93 | 273.37 | 16.36 |
| | P2 | -76.29 | 233.30 | 273.19 | 17.10 |
| | P3 | -79.10 | 237.07 | 277.19 | 16.92 |
| | P4 | -80.12 | 236.94 | 277.16 | 16.97 |
| Area 2 | P5 | -86.96 | 91.43 | 131.29 | 43.59 |
| | P6 | -87.52 | 55.90 | 93.28 | 66.87 |
| | P7 | -87.59 | 82.21 | 122.16 | 48.59 |
| | P8 | -89.85 | 48.10 | 83.59 | 73.80 |
| | P9 | -91.82 | 37.35 | 65.67 | 75.83 |
| | P10 | -102.28 | 10.93 | 29.43 | 169.41 |
| Area 3 | P11 | -102.97 | 10.69 | 28.33 | 165.08 |
| | P12 | -110.52 | 1.78 | 7.31 | 310.27 |
| | P13 | -110.77 | 1.74 | 7.64 | 339.57 |
| | P14 | -112.03 | 1.03 | 7.90 | 668.75 |
| | P15 | -112.98 | 1.10 | 5.52 | 403.73 |

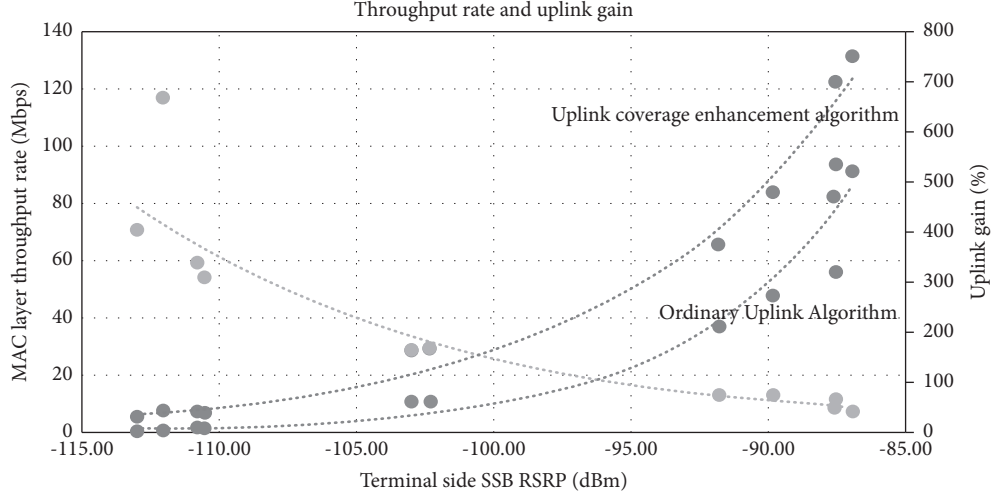


FIGURE 8: Throughput and gain analysis.

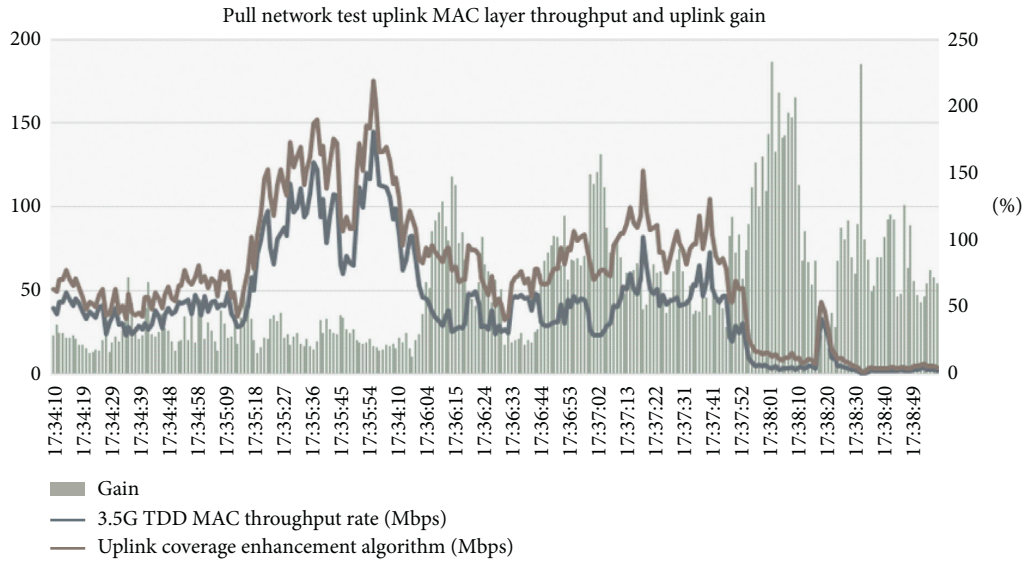


FIGURE 9: MAC layer throughput rate and super-uplink gain analysis.

4.3. Pull Net Test. By testing the highest and lowest platform routes, the test results of the uplink coverage enhancement algorithm are as shown in Figure 9. It can be seen that after the uplink coverage enhancement algorithm is executed, the average uplink rate increase ratio reaches 20% to 40%.

5. Conclusion

This paper designs a 5G network-based uplink coverage enhancement algorithm. Through the superposition of C-band spectrum and Sub-3G uplink spectrum, it greatly increases the uplink spectrum resources and improves the user capacity and experience of the 5G network. Tests have proved that the algorithm can solve the 5G uplink and downlink coverage problems and increase the rate of edge users, which is evolutionary. With the gradual recultivation of existing frequency bands, the available frequency bands

for 5G will be more abundant and multiband carrier aggregation and collaborative networking will be more widely used, providing a better user experience.

Data Availability

The data used to support the findings of this study are included within the article.

Conflicts of Interest

The authors declare no conflicts of interest.

Acknowledgments

This work was funded by the QingLan Project of Jiangsu Province (202010).

References

- [1] B. Mengesha, P. T. Ferrera, and R. Gaudino, "Analysis of 5G new radio uplink signals on an analogue-RoF system based on DSP-assisted channel aggregation," *Applied Sciences*, vol. 9, no. 1, 2018.
- [2] B. Lahad, M. Ibrahim, S. Lahoud, K. Khawam, and S. Martin, "Joint modeling of TDD and decoupled uplink/downlink access in 5G HetNets with multiple small cells deployment," *IEEE Transactions on Mobile Computing*, vol. 20, 2020.
- [3] H. Uzawa, K. Honda, H. Nakamura et al., "Dynamic bandwidth allocation scheme for network-slicing-based TDM-PON toward the beyond-5G era," *Journal of Optical Communications and Networking*, vol. 12, no. 2, pp. A135–A143, 2019.
- [4] N. Zhang, J. Wang, G. Kang, and Y. Liu, "Uplink non-orthogonal multiple access in 5G systems," *IEEE Communications Letters*, vol. 20, no. 3, pp. 458–461, 2016.
- [5] R. P. Verdecia and J. I. Alonso, "Performance analysis of two-hop mmWave relay nodes over the 5G NR uplink signal," *Applied Sciences*, vol. 11, no. 13, p. 5828, 2021.
- [6] H. Shen, Q. Ye, W. Zhuang, W. Shi, G. Bai, and G. Yang, "Drone-small-cell-assisted resource slicing for 5G uplink radio access networks," *IEEE Transactions on Vehicular Technology*, vol. 70, no. 7, 2021.
- [7] M. A. Lema, E. Pardo, O. Galinina, S. Andreev, and M. Dohler, "Flexible dual-connectivity spectrum aggregation for decoupled uplink and downlink access in 5G heterogeneous systems," *IEEE Journal on Selected Areas in Communications*, vol. 34, no. 11, pp. 2851–2865, 2016.
- [8] X. Li, Z. Zhong, Y. Niu, and H. Zhou, "Backoff HARQ for Contention-Based Transmission in 5G Uplink," in *Proceedings of the 4th EAI International Conference, IoTaaS 2018*, Xian, China, vol. 7, pp. 284–291, November 2019.
- [9] W. Tang, S. Kang, B. Ren, X. Yue, and X. Zhang, "Uplink pattern division multiple access in 5G systems," *IET Communications*, vol. 12, no. 9, pp. 1029–1034, 2018.
- [10] S. Sun, S. Moon, and J. K. Fwu, "Practical link adaptation algorithm with power density offsets for 5G uplink channels," *IEEE Wireless Communication Letters*, vol. 9, 2020.
- [11] B. K. Letaief, P. Fan, Z. Chen, and Y. Dong, "Mobility-Aware Uplink Interference Model for 5G Heterogeneous Networks," *IEEE transactions on wireless communications*, vol. 15, 2016.
- [12] G. Celik and H. Celebi, "TOA Positioning for Uplink Cooperative NOMA in 5G networks," *Physical Communication*, vol. 36, 2019.